



Research on the Monocular Ranging Method of the Leading Vehicle in Multi-weather

Yong Tian¹, Quancai Li^{1*}, Shuman Guo¹, Gongrou Fu¹, Shichang Wang¹
and Junkai Guo¹

¹School of Mechanical Engineering, North China University of Water Resources and Electric Power, Zhengzhou, 450045, China.

Authors' contributions

This work was carried out in collaboration among all authors. Author YT designed the study, performed the statistical analysis, wrote the protocol, and wrote the first draft of the manuscript. Authors QL and SG managed the analyses of the study. Author GF, SW and JG managed the literature searches. All authors read and approved the final manuscript.

Article Information

DOI: 10.9734/JSRR/2021/v27i530390

Editor(s):

(1) Prof. Cheng-Fu Yang, National University of Kaohsiung, Taiwan.

Reviewers:

(1) Stefan Tabacu, University of Pitesti, Romania.

(2) Saket Sinha, The University of Sydney, Australia.

Complete Peer review History: <http://www.sdiarticle4.com/review-history/69993>

Original Research Article

Received 17 April 2021
Accepted 23 June 2021
Published 28 June 2021

ABSTRACT

In order to improve the accuracy of the monocular distance measurement of the vehicle in front under sunny, cloudy, rainy, snowy, and foggy weather, an improved pixel-mapping monocular distance measurement method is proposed. This method is based on eight-connected domains to detect the front vehicle, obtain the line pixels of the target vehicle in the image, and fit the image line pixels to the corresponding real longitudinal distance function, and combine the fitted function with the internal and external parameters of the camera. An improved pixel-mapping monocular ranging model is obtained. Set up a test environment under different weather to verify the feasibility of the algorithm. The results show that in the four environments, the detectable distances are within 70m, 60m, 30m, and 40m respectively; the error of the improved pixel-mapping monocular ranging method is reduced by 0.6% on average compared with before the improvement, up to 0.92% ; The improved algorithm ranging errors under the four weathers are 1.8513%, 2.6987%, 4.0137%, and 2.5795% respectively, which achieves the purpose of improving the accuracy of the monocular distance measurement of the vehicle in front under multiple weather conditions.

*Corresponding author: E-mail: 838846263@qq.com;

Keywords: Multi-weather; front vehicle; monocular ranging; pixel mapping.

1. INTRODUCTION

With the increase of vehicle ownership and the increase of vehicle rear end accidents, road traffic safety has been paid more and more attention. In view of the road traffic safety, each vehicle enterprise also continuously improves the investment in the research of advanced driving assistance system. In the advanced driving assistance system, the detection and ranging of the vehicles in front is very important. The detection and ranging of the vehicles in front of the vehicle based on monocular vision has also been widely concerned.

The existing monocular ranging methods mainly include frame difference based ranging, pixel mapping based ranging, and geometric relationship based ranging [1].

Some scholars start their research based on the difference between two frames of images. Su Ping et al. [2] calculated the distance between the target and the camera through geometric calculation based on the position difference of the target in the two frames of the image, combined with the actual movement speed of the target. Zhou Dongsheng et al. [3] made a camera motion guide rail model, which allowed the camera to move on the guide rail, and calculated the distance of the target object by comparing two frames of images of the camera at different positions. The algorithm error based on frame difference ranging is too large and not suitable for car driving with high safety requirements;

Some scholars focus on pixel mapping ranging as research. Yeong P et al. [4][5] extract distance information by establishing a mapping relationship between row pixel values and actual distances. Bao et al. [6] [7] proposed a monocular vision vehicle ranging method based on the linear relationship between the average length of the vehicle width and the actual distance of the detected vehicle. Zhang Y et al. [8][9] used the constraint condition of parallel lane lines to select the points of the lane lines in the image, and obtained the coordinates of the corresponding points on the plane through derivation of the set, so as to realize the distance measurement of obstacle vehicles. The distance measurement based on pixel mapping is simple and does not require calibration of the internal and external parameters of the camera, but only

the relationship between the axial distance of the camera and the row pixels can be obtained.

Some scholars have conducted research on the principle of pixel triangles. KIM G et al. [10] used the actual vehicle width of the target vehicle to conduct distance measurement, and obtained the distance of the target object according to the geometric transformation of similar triangles. Ye Q et al. [11] obtained the area of the license plate of the vehicle ahead in the image through image processing, and combined the real area of the license plate and the principle of small hole imaging to obtain the distance between the target and the camera. Ranging based on geometric relationships requires known and accurate camera internal and external parameters, which has strong practicability and portability, but it is difficult to extract them from the image for rainy, snowy, and foggy weather with low visibility. The characteristic information of the target vehicle.

At the same time, most of the monocular ranging methods are only limited to sunny days, without considering the influence of rain, snow, fog and other weather. In this paper, an improved pixel mapping method is proposed by combining pixel mapping ranging with geometric relation ranging, and the feasibility and effectiveness of the algorithm are verified in sunny, rainy, snowy and foggy weather environment, so as to achieve the purpose of improving the monocular ranging accuracy of vehicles in front in multi weather.

2. TARGET VEHICLE DETECTION

For target vehicle ranging, target vehicle detection is the basis and guarantee of ranging accuracy. In this paper, connected domain segmentation method combined with local adaptive threshold method is used to process the image to get the target vehicle information. The processing flow is shown in Fig. 1.

2.1 Construction of System Coordinate System

In this paper, the test scenarios of road, vehicle and monocular camera are built in the simulation software PreScan, as shown in Fig. 2a. The location of the monocular camera is taken as the coordinate origin of the ranging model, and the system coordinate system is shown in Fig. 2b.

2.2 Target Vehicle Image Preprocessing

2.2.1 Target vehicle region of interest selection

Target Vehicle Area of Interest Pick the image of the front vehicle taken by the camera as shown in Fig. 2c.

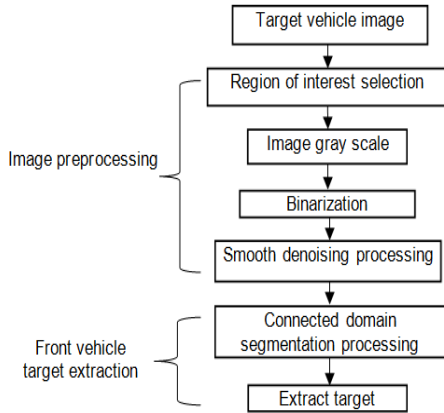


Fig. 1. Flow chart of vehicle detection

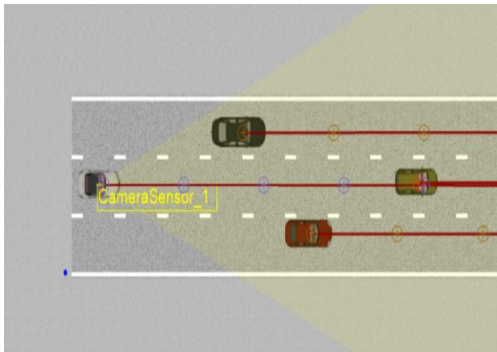


Fig. 2a. Simulation scene building diagram

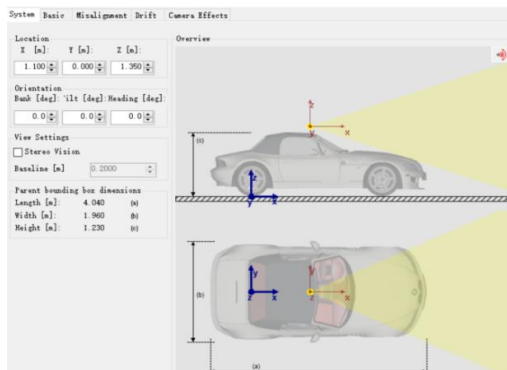


Fig. 2b. System coordinate system



Fig. 2c. Original vehicle image

This article uses MATLAB Vision Toolbox to process images. The original image of the vehicle in front of Fig. 2c. In the original image, the environment around the target vehicle is a disturbing factor, which is not conducive to extracting the target vehicle. Setting the target vehicle's region as the area of interest, selecting a frame and processing only the area of interest can effectively reduce the processing difficulty and improve the operation speed. In this paper, the sky part of the image is removed, and the rest is the area of interest, as shown in Fig. 3a.

2.2.2 Target vehicle gray scale processing

The image taken by the monocular camera is a color image, and each pixel of the color image is determined by the three component values of R, G, and B. It is particularly complicated to process the color image directly. Combine the three component values of the color image to obtain a gray-scale image with the same three components of R, G, and B. The gray-scale image can greatly improve the image processing speed. The gray scale processed image is shown in Fig. 3b, and the processed pixel gray scale value is shown in the following formula:

$$\begin{cases} f(x, y) = R(x, y) \\ f(x, y) = G(x, y) \\ f(x, y) = B(x, y) \end{cases} \quad (1)$$

2.2.3 Target vehicle binarization processing

Each pixel of the gray scale image is composed of 0 to 255. Each pixel is set with a threshold T, and the gray scale image is divided according to the threshold T. The area greater than the threshold T is set to white (the gray scale value is 255), which is less than The area of the threshold T is set to black (the gray value is 0), so that a

black and white target and background are obtained. The formula is as follows:

$$f(x,y) = \begin{cases} 0 & f(x,y) < T \\ 255 & f(x,y) > T \end{cases} \quad (2)$$

There are generally two common methods for binarization algorithms, one is the global threshold method, and the other is the local adaptive threshold method. The global threshold method directly processes the entire image according to a fixed threshold T ; the local adaptive threshold method divides the entire image into several blocks, and then processes each block separately, matching the appropriate threshold according to the different pixel values in each area.



Fig. 3a. Region of interest image

In this paper, for the extraction of vehicles in front of different weather, the environment is more complicated, and only using the global threshold cannot get good processing results. Therefore, this paper adopts the local adaptive threshold method for image binarization. The processing result is shown in Fig. 3c.

In the image obtained by the binarization process, the target vehicle is a black area. However, in the subsequent target vehicle extraction, the white highlight area of the image is processed. In this paper, the binary image is reversed, and the target vehicle is converted from black and white to the background. Fig. 3d shows the image inversion processing diagram.

2.2.4 Smooth denoising processing

Since the image processed by local adaptive threshold binarization is processed according to each area, the non-target area in the image will also have some highlight areas, which will affect the subsequent target extraction. In this paper, the threshold T_s is set according to the area size S of the white highlight area, and T_s is set to 100 in this paper, and the highlight areas with an area

less than 100 are eliminated as interference factors. The processing formula is as follows:

$$f(x,y) = \begin{cases} 0 & T_s < 100 \\ 255 & T_s > 100 \end{cases} \quad (3)$$

The processing result is shown in Fig. 3e.



Fig. 3b. Gray scale rendering



Fig. 3c. Binary processing diagram



Fig. 3d. Image inversion rendering

2.3 Front Vehicle Target Extraction

In an image, when two pixels are adjacent to each other, it is said that the two pixels are connected. There are two common connection methods: 4-connectivity and 8-connectivity. Four-connectivity means that pixels are adjacent in four directions: up, down, left, right, upper left, upper-right, lower-left, and lower-right, as shown in Fig. 4. Connected domain adjacency graph.

This paper extracts the preceding vehicle based on the eight-connected domain. The extracted target vehicle is framed in the original image. The extraction result is shown in Fig. 5.

3. TARGET VEHICLE RANGING

The existing monocular ranging methods mainly include ranging based on frame difference, ranging based on pixel mapping, and ranging based on geometric relationship. This paper adopts the pixel mapping method and combines geometric relationship distance measurement, and proposes an improved pixel mapping method to measure the target vehicle distance.

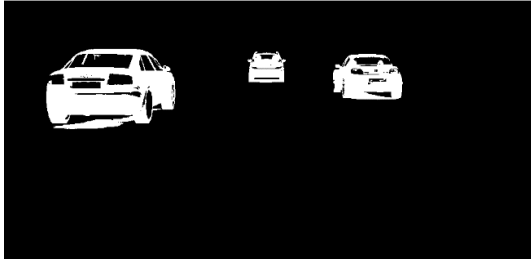


Fig. 3e. Smooth denoising effect picture

3.1 Pixel Mapping Principle

The existing monocular ranging methods mainly include ranging based on frame difference, ranging based on pixel mapping, and ranging based on geometric relationship. This paper adopts the pixel mapping method and combines geometric relationship distance measurement, and proposes an improved pixel mapping method to measure the target vehicle distance.

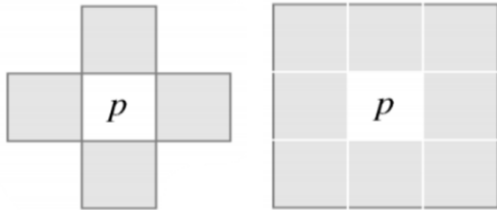


Fig. 4. Connected domain adjacency graph

The imaging of the monocular camera conforms to the principle of small hole imaging. Fig. 6a shows the imaging model of the monocular camera. A is the actual object, the height is H meters, a is the image formed in the camera, the height is h meters, f is the focal length of the camera, and L is the distance between the object and the optical axis of the camera.

Using the triangle similarity principle, the relationship between the actual object and the

camera imaging can be obtained, as shown in the following formula:

$$\frac{L}{f} = \frac{H}{h} \quad (4)$$

Since the focal length f is a fixed parameter of the camera, and L, H, and h are all unknown, the expression of the actual distance L can be obtained:

$$L = f(H, h) \quad (5)$$

If the height H of the object is known, the actual distance L is only related to the height h of the object in the image. As L changes, the corresponding line pixel u of a certain point of the object changes in the image. As shown in Fig. 6b, in the same horizontal plane, different L (L1 and L2) correspond to different rows of pixels u in the image.



Fig. 5. Front vehicle detection map

Then the L expression can be simplified to the expression with the row pixel u:

$$L = f(u) \quad (6)$$

By counting the distance L corresponding to each row of pixels, the relationship between the row of pixels and the distance L can be obtained. Some calibration targets are made in PreScan, and the actual distance between the row pixels at the bottom of each calibration target in the image and its distance is calculated. The statistical results are shown in Table 1.

Use the cftool toolbox in MATLAB to fit the data in Table 1, The fitted curve is shown in Fig. 7 and get the following formula:

$$L = 2.879 \times e^{0.005988u} + 5.139 \times 10^{-7} \times e^{0.05398u} \quad (7)$$

The above fitting formula is the distance measurement model of the pixel mapping method. According to the pixel row coordinate u of the bottom of the target vehicle in the image, the distance L of the target vehicle from the camera is obtained.

The distance between the target and the camera obtained by pixel fitting is the distance in the optical axis direction, and there is no lateral distance. The measured distance for the vehicle in front of the side lane is not accurate. In order to solve this problem, this paper proposes an improved pixel mapping ranging

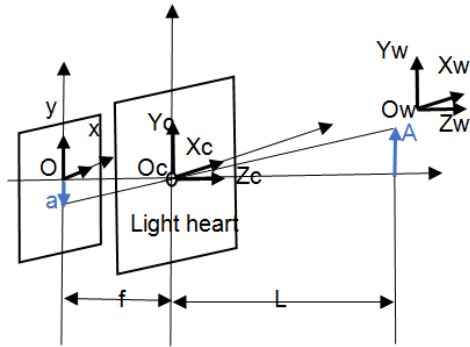


Fig. 6a. Monocular camera imaging model

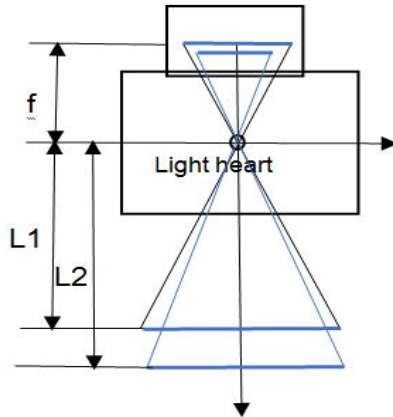


Fig. 6b. Pixel mapping model diagram

3.2 Improved Pixel Mapping Ranging

The improved pixel mapping ranging is based on the pixel mapping ranging, combined with the camera internal parameter calibration, through the transformation matrix after calibration, the image coordinate transformation is carried out,

and the actual distance between the target and the camera is obtained.

Image coordinate conversion generally requires three coordinate systems, image pixel coordinate system (O-xy), camera coordinate system (Oc-XcYcZc), world coordinate system (Ow-XwYwZw), from the image pixel coordinate system to the camera coordinate system mutual. The conversion requires the camera's internal parameter matrix $[I]$, and the mutual conversion between the camera coordinate system and the world coordinate system requires an external parameter matrix including translation and rotation $[M]$. The conversion process is shown in the following formula:

$$Z_c \begin{bmatrix} x \\ y \\ 1 \end{bmatrix} = \begin{bmatrix} \frac{f}{dx} & 0 & x_0 \\ 0 & \frac{f}{dy} & y_0 \\ 0 & 0 & 1 \end{bmatrix} * \begin{bmatrix} X_c \\ Y_c \\ Z_c \end{bmatrix} = [I] * \begin{bmatrix} X_c \\ Y_c \\ Z_c \end{bmatrix} \quad (8)$$

$$Z_c \begin{bmatrix} x \\ y \\ 1 \end{bmatrix} = \begin{bmatrix} \frac{f}{dx} & 0 & x_0 & 0 \\ 0 & \frac{f}{dy} & y_0 & 0 \\ 0 & 0 & 1 & 0 \end{bmatrix} * \begin{bmatrix} r_{11} & r_{12} & r_{13} & t_1 \\ r_{21} & r_{22} & r_{23} & t_2 \\ r_{31} & r_{32} & r_{33} & t_3 \\ 0 & 0 & 0 & 1 \end{bmatrix} * \begin{bmatrix} X_w \\ Y_w \\ Z_w \\ 1 \end{bmatrix} = [I] * [M] * \begin{bmatrix} X_w \\ Y_w \\ Z_w \\ 1 \end{bmatrix} \quad (9)$$

The camera used in this article is placed horizontally forward, with the optical center position O_c as the origin of the world coordinate system, and the camera coordinate system overlaps the world coordinate system, so the world coordinates can be replaced by camera coordinates [12].

Make a 10*8 black and white checkerboard target in PreScan, use the camera to take images of the target from various angles, and use the toolbox in MATLAB for calibration. The spatial angle distribution diagram of the target calibrated by the camera is shown in Fig. 8.

Through internal parameter calibration, the internal parameter matrix of the camera is as follows:

$$[I] = \begin{bmatrix} 1124.5 & 0 & 480.4 \\ 0 & 1124.5 & 360.6 \\ 0 & 0 & 1 \end{bmatrix} \quad (10)$$

Thus, the conversion relational expression from the pixel coordinate system to the camera coordinate system can be obtained:

$$\begin{bmatrix} X_c \\ Y_c \\ Z_c \end{bmatrix} = Z_c * [I]^{-1} * \begin{bmatrix} x \\ y \\ 1 \end{bmatrix} \tag{11}$$

Zc can be obtained from the fitting formula of the pixel mapping method, the formula is as follows:

$$ZC=L=2.879E^{0.005988X}+5.139 \times [10]^{(-7)} \times E^{0.05398X} \tag{12}$$

Combining formula (11) and formula (12) can get the following formula:

$$\begin{bmatrix} X_c \\ Y_c \\ Z_c \end{bmatrix} = L * [I]^{-1} * \begin{bmatrix} x \\ y \\ 1 \end{bmatrix} \tag{13}$$

In the camera coordinate system, the optical center of the camera is the origin of the coordinate. In the monocular distance measurement of the front vehicle, only the horizontal distance is considered, and the longitudinal distance is not considered. Then the distance from the target to the camera is as follows:

$$L_c = \sqrt{X_c^2 + Z_c^2} \tag{14}$$

4. TEST VERIFICATION AND RESULT ANALYSIS

Set up four types of weather in PreScan: sunny, cloudy, rainy, snowy, and foggy to test the detection and ranging effect of the vehicle on the front target vehicle under different weather under the same road conditions.

Both the test car and the target car move forward at a certain speed. Fig. 9 shows the detection

images at three times of 1s, 4s, and 7s under four types of weather. The actual distances of the three targets in 1s are 15.70m, 38.43m, and 20.74m, and the actual distances of the three targets in 4s. They are 24.59m, 60.06m, 25.22m, and the actual distances of the three targets in 7s are 29.85m, 71.68m, and 27.94m.

As shown in the Fig.9., in a sunny environment, the detection effect within 70m is good; in a cloudy or rainy environment, the field of view is relatively limited, the detection effect is good within 60m, and the detection effect around 70m is poor, and only part of the outline of the target vehicle can be obtained; In a snowy environment, the detection effect is good within 30m, and the detection is invalid if it is greater than 30m; in a foggy environment, the detection effect is good within 40m, and the detection is invalid if it is greater than 40m.

The detected targets are measured by two ranging algorithms. The detected targets are named'target one','target two', and'target three' from left to right. The ranging results and errors under three types of weather are shown in the figure Shown.

This article defines the ratio of the difference between the measured distance and the true distance to the true distance as the error. The improved algorithm takes into account the lateral distance of the target. When the target is directly in front, the lateral distance is 0, and the results of the two algorithms are basically the same; when the target is not directly in front, the accuracy of the improved algorithm is higher due to the influence of the lateral distance.

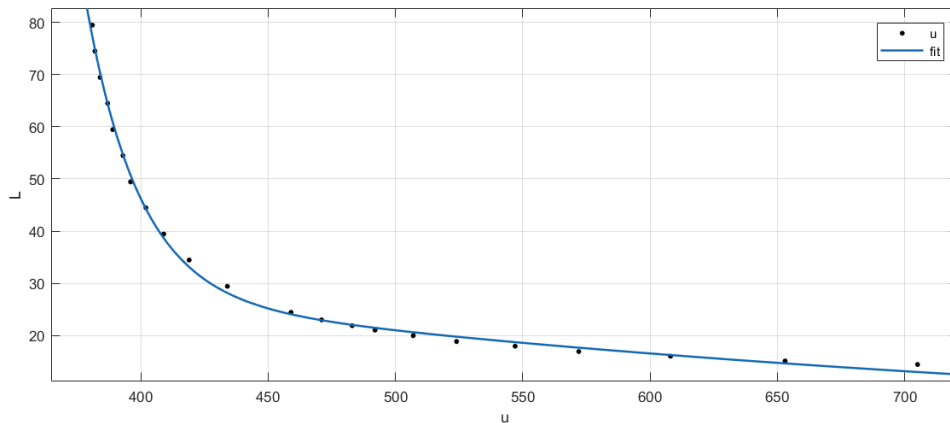


Fig. 7. Fitting curve graph

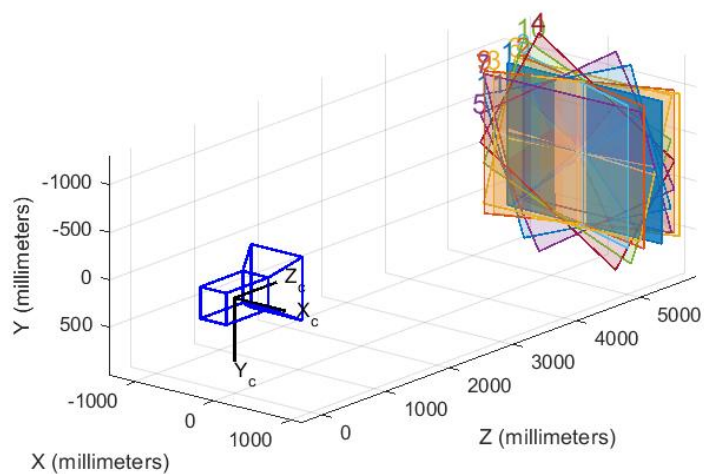


Fig. 8. Camera internal parameter calibration

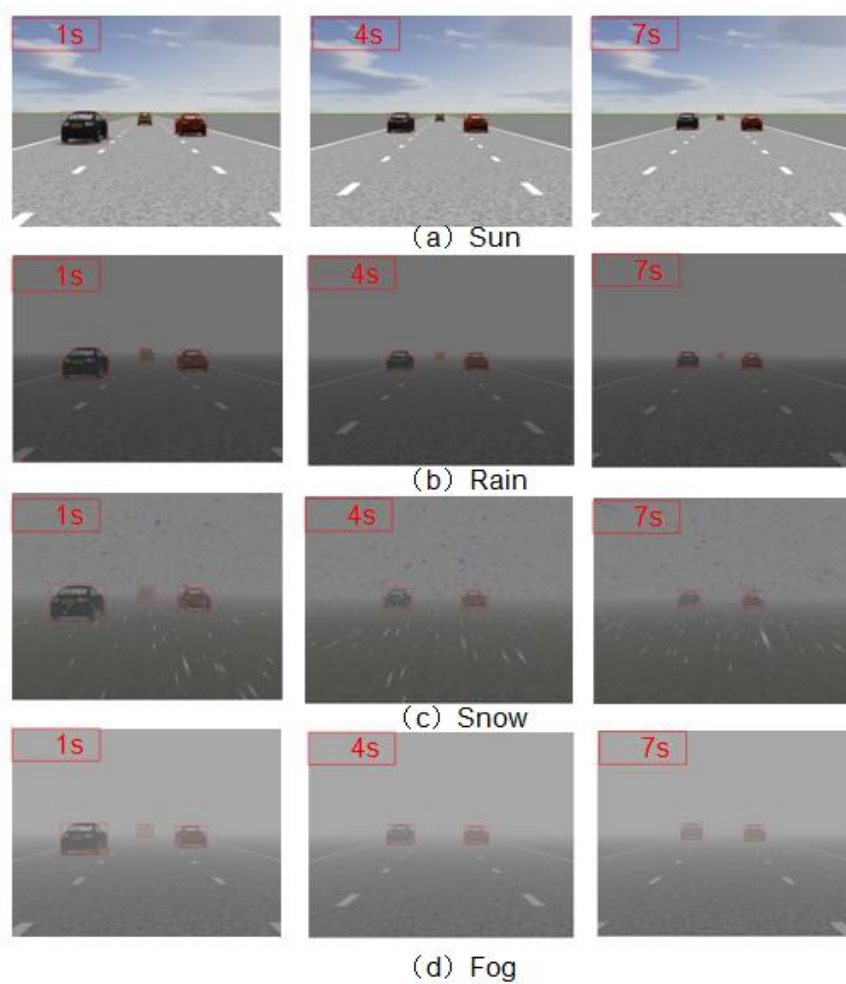


Fig. 9. 1s, 4s, 7s test results in four weather conditions

Table.1. Comparison table of row pixels and true distance

True distance L/m	Line pixels u/pixel	True distance L/m	Line pixels u/pixel
14.49	705	29.45	434
15.16	653	34.48	419
16.08	608	39.45	409
16.96	572	44.48	402
18.00	547	49.45	396
18.89	524	54.48	393
20.01	507	59.45	389
21.08	492	64.48	387
21.93	483	69.45	384
23.03	471	74.48	382
24.48	459	79.45	381

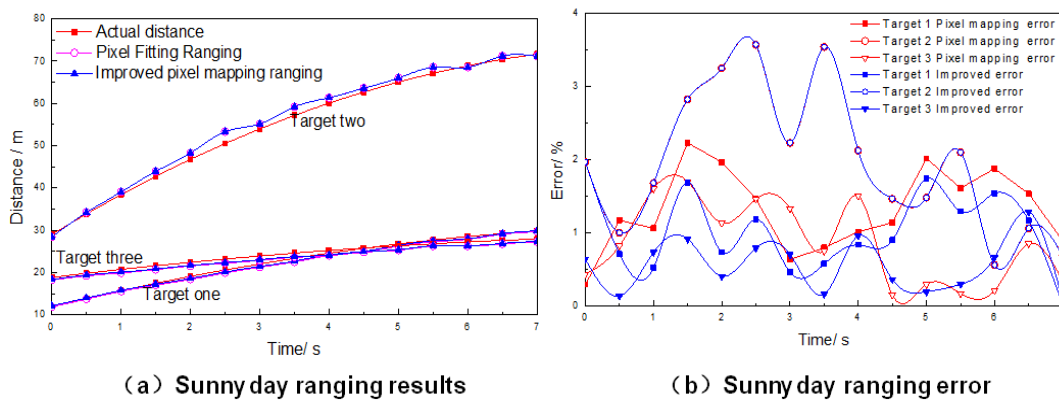


Fig. 10. Ranging results and errors on sunny days

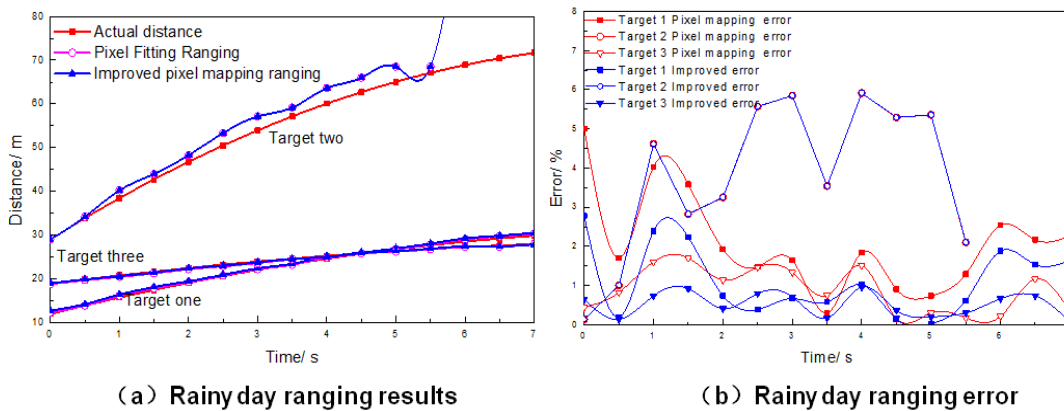


Fig. 11. Ranging results and errors on rainy day

It can be seen from Fig 10 to Fig 13 that the improved algorithm is significantly better than the pixel mapping method for the distance measurement of the target one and the target two. The target three is directly in front of the camera, and the ranging results of the two algorithms are basically the same. In different

weather, the ranging effect is good within 70 meters on a sunny day, within 60 meters on a cloudy and rainy day, and within 30 meters on a snowy day. The maximum error is less than 6% within the effective ranging range. Table 2 shows the statistics of the ranging error under the three types of weather.

It can be seen from Table 2 that the overall error of the improved algorithm is smaller than the error before the improvement, and the error is reduced by 0.6% on average, especially in rainy and snowy days, the effect of the improved algorithm is more obvious, and the error is reduced by about 1% in sunny, cloudy and rainy

days. Under the four weather scenarios of sky, snow and fog, the average errors are 1.8513%, 2.6997%, 4.0137%, and 2.5795%, respectively, which are lower than the relative error of traditional monocular ranging of 4.9% calculated in the literature [13].

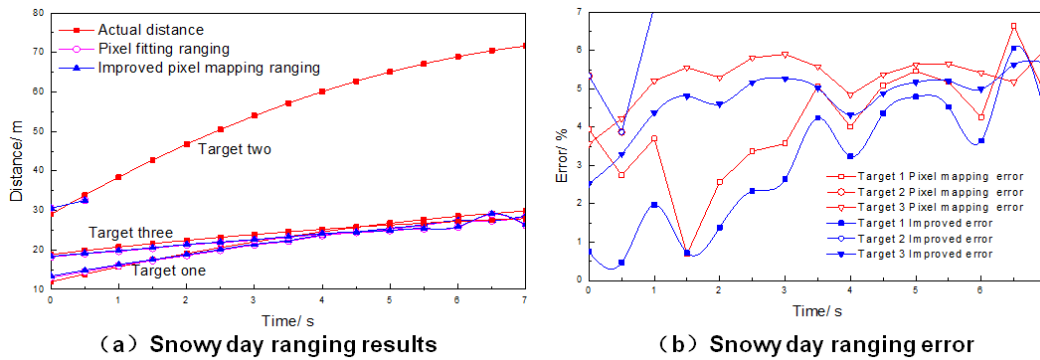


Fig. 12. Ranging results and errors on snowy day

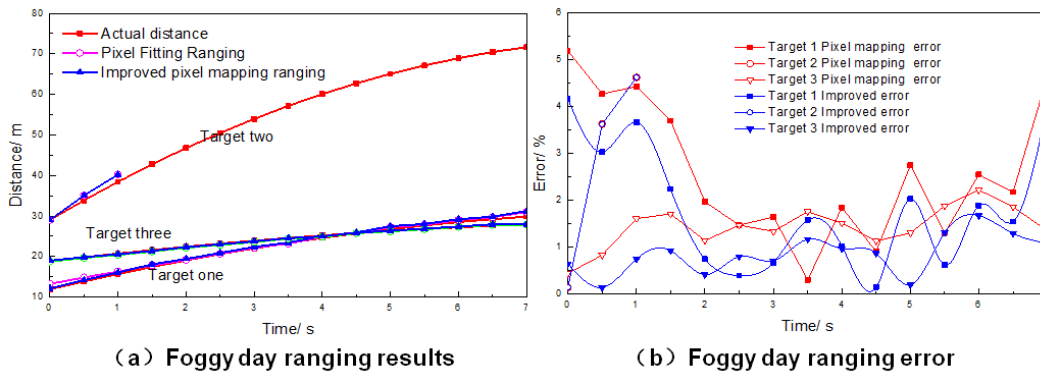


Fig. 13. Ranging results and errors on foggy day

Table 2 Error statistics table

Weather	Model	Measuring range /m	Error/%	average error /%
Sunny	Pixel mapping ranging	0-30	1.9124	2.0076
		30-70	2.1028	
	Improved ranging	0-30	1.2891	1.6950
		30-70	2.1009	
Rainy	Pixel mapping ranging	0-30	2.4837	3.1350
		30-70	3.7864	
	Improved ranging	0-30	1.8206	2.4987
		30-70	3.1769	
Snowy	Pixel mapping ranging	0-30	4.9457	4.9457
	Improved ranging	0-30	4.0137	4.0137
Foggy	Pixel mapping ranging	0-30	1.9202	3.0182
		30-40	4.1162	
	Improved ranging	0-30	1.6428	2.5795
		30-40	3.5162	

5. CONCLUSION

This paper proposes an improved pixel-mapping monocular ranging method, which can realize the monocular ranging of the front vehicle under four weathers: sunny, cloudy, rainy, snowy, and foggy. Through the algorithm verification and result analysis, we can get:

- (1) For the four environments of this article, sunny, cloudy, rainy, snowy, and foggy, the visibility of the camera is different, and the detectable distance is within 70m, 60m, 30m, and 40m respectively;
- (2) Compared with the original method, the improved algorithm considers the lateral distance of the front target vehicle, which effectively reduces the measurement error. The error of the improved pixel-mapping monocular ranging method is reduced by 0.6% on average compared with before the improvement, up to 0.93%;
- (3) Within the effective ranging range of sunny, cloudy, rainy, snowy, and foggy, the improved algorithm's ranging error varies with visibility, respectively 1.8513%, 2.6987%, 4.0137%, 2.5795%, which are all lower than the traditional The relative error of monocular ranging is 4.9%, which satisfies the purpose of improving the accuracy of monocular ranging of the preceding vehicle in multiple weather.

ACKNOWLEDGEMENTS

This project is supported by the Henan University Science and Technology Innovation Team Support Program: Research on Optimal Control of Hydrogen Fuel Vehicle Power System (19IRTSTHN011).

COMPETING INTERESTS

Authors have declared that no competing interests exist.

REFERENCES

1. Han XJ. Research on UAV ranging algorithm based on monocular vision [J]. Reliability and environment test of electronic products. 2019;37(3):54-57
2. Su P, Zhu XH. Research on water surface target recognition and ranging based on monocular vision [J]. Computer technology and development. 2021;31(02):80-84
3. Zhou DX, Han DS. Pseudo binocular dynamic ranging method based on Monocular Video [J]. Electronic measurement technology. 2021;44(03):38-44
4. Ki Yeong P, Sun YoungH Robust Range Estimation with a Monocular Camera for Vision – Based Forward Collision Warning System [J]. The Scientific World Journal. 2014;2014:1–9.
5. Han J, Heo O, Park M, et al. Vehicle distance estimation using a mono – camera for FCW / AEB systems [J]. International Journal of Automotive Technology, 2016;17(3):483 – 491.
6. Bao D, Wang P. Vehicle distance detection based on monocular vision[C]// International Conference on Progress in Informatics and Computing. IEEE. 2017;187-191.
7. Xu Z , Wang L , Jie W . A Method for Distance Measurement of Moving Objects in a Monocular Image[C]// 2018 IEEE 3rd International Conference on Signal and Image Processing (ICSIP). IEEE; 2018.
8. Zhang Y, Wang Guili, Zhou Xuting, et al. Ranging algorithm based on monocular vision[J]. Computer and Digital Engineering, 2020;48;(364)(02):91-95.
9. Chen LG, Li K, Zhang Z, Yu H, Wang X. Target ranging algorithm based on computer vision [J]. Journal of missile and guidance, 2020;40(02):93-96.
10. KIM G, CHO J S. Vision – based vehicle detection and inter – vehicle distance estimation for driver alarm system[J]. Optical Review. 2012;19(6):388 – 393.
11. Ye Q. Analysis of Front Vehicle Detection and Ranging Based on Computer Vision[J]. Journal of Lanzhou Institute of Technology. 2019;26(05):79-83.
12. Yu H, Zhang W. Measurement method of car following distance based on monocular vision [J] . Journal of Southeast University (NATURAL SCIENCE EDITION), 2012;42(3):542-546.

13. Xu C, Gao M, Cao H. Tank target ranging method based on attitude angle estimation in monocular image [J]. Acta PHOTONICA Sinica, 2015;44(5):1-8.

© 2021 Tian et al.; This is an Open Access article distributed under the terms of the Creative Commons Attribution License (<http://creativecommons.org/licenses/by/4.0>), which permits unrestricted use, distribution, and reproduction in any medium, provided the original work is properly cited.

Peer-review history:
The peer review history for this paper can be accessed here:
<http://www.sdiarticle4.com/review-history/69993>